Supplementary Material

Text S1 Chemicals and reagents

Chloronitromethane (CNM; GC, 96.5%), dichloronitromethane (DCNM; GC, 98.5%), trichloronitromethane (TCNM; GC, 97%), bromonitromethane (BNM; GC, 97%), dibromonitromethane (DBNM; GC, 97%), tribromonitromethane (TBNM; GC, 100%), bromochloronitromethane (BCNM; GC, 97%), bromochloronitromethane (BDCNM; GC, 97%), and dibromochloronitromethane (DBCNM; GC, 97.4%) were purchased from Quality Control Chemicals (USA). Methyl tert-butyl ether (MTBE; GC, ≥99.9%) was purchased from Aladdin (China). Ammonium sulfate ($(NH_4)_2SO_4$; 99%) was purchased from Fuchen (China). Aspartic acid (≥99%), sodium bromide (NaBr; 99%), sodium thiosulfate ($Na_2S_2O_3$; ≥99%), disodium phosphate (Na_2HPO_4; 99%), and sodium dihydrogen phosphate (NaH_2PO_4; 99%) were purchased from Sinopharm (China). Sodium hypochlorite (NaOCl, 5%), copper sulfate ($CuSO_4$; 99%) was purchased from Sigma-Aldrich (China), and NaOCl was used to prepare free chlorine solution. All chemicals and reagents were of analytical grade at least and used without further purification.

Text S2 Determination of HNMs concentrations

The concentrations of HNMs were analyzed by GC-ECD (Agilent 7890B, USA) equipped with an HP-1 column (30 m × 0.32 mm × 0.25 μm). The oven temperature program was an initial temperature of 30℃ for 6 min and ramped up to 100℃ at 15℃/min for 5 min, followed by ramping up to 240℃ at 35℃/min for 5 min. 1 μL sample was injected in spitless mode. The carrier gas was ultra-high purity (UHP) helium at 1.2 mL/min, and the make-up gas was UHP nitrogen at 60 mL/min. The injection and GC-ECD temperatures were 117℃ and 280℃, respectively.

Text S3 The analytical methods for intermediates

The analysis of intermediates was performed using a gas chromatograph-quadrupole mass spectrometer (GC-MS; Agilent 7890A GC, 5975 MS, USA) equipped with an HP-5m separation

column (30 m × 0.25 mm, 0.25 μm). The temperature program consisted of an oven temperature of 40℃ for 2 min, followed by ramping to 300℃ at 40℃/min and held for 5 min. The temperature of the injection port was set at 300℃, and the detector temperature was set at 280℃. The injection volume (1 μL) was carried by a helium gas with a constant flow rate of 1.0 mL/min. The MS was operated in the total ion chromatogram mode and selected ion monitoring mode.

Text S4 Calculation of bromine incorporation factors (BIFs) and bromine utilization factors (BUFs)

The values of BIF and BUF were calculated by the following equations (Eqs. (S1) and (S2)):

$$BIF = \frac{[BNM]+[BCNM]+[BDCNM]+2[DBNM]+2[DBCNM]+3[TBNM]}{[HNMs]}, \quad (S1)$$

$$BUF = \frac{[BNM]+[BCNM]+[BDCNM]+2[DBNM]+2[DBCNM]+3[TBNM]}{[Br^-]}, \quad (S2)$$

All concentrations are on the molar basis.

Text S5 Different forms of chlorine during LED-UV_{265}/chlorine disinfection

As shown in Fig. S7, during LED-UV_{265}/chlorine disinfection with ASP, the total chlorine gradually decreased from 10.36 to 1.05 mg/L with reaction time. The free chlorine concentration decreased rapidly from 10.19 to 1.79 mg/L in the initial 1 min, and then decreased slowly to 0.08 mg/L at 9 min. The experimental results suggest that the free chlorine is rapidly consumed and converted to combined chlorine during the reaction process. One part of this is probably due to the reaction of ASP and HClO to form organic chloramine (Eq. (S3)); the other part is probably due to the reaction of ammonia nitrogen released from amino acids and HClO to form inorganic chloramine (Eq. (S4)) (How et al., 2017). In addition, the total chlorine concentration decreased gradually with reaction time, which could be due to the continued reaction of the organic chloramine to form DBPs such as HNMs.

$$R\text{-}NH_2 + HClO \rightarrow R\text{-}NHCl + H_2O \quad (S3)$$

$$NH_3 + HClO \rightarrow NH_2Cl + H_2O \quad (S4)$$

Table S1 Physical and chemical properties of nine HNMs.

Compounds	Abbreviation	Structure	Weight	pKa	Boiling point (℃, 101.325 kpa)	Solubility (mg/L, 20℃)
Chloronitromethane	CNM	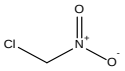	95.5	7.30	122.5	32020
Dichloronitromethane	DCNM	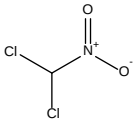	130	5.97	107	11750
Trichloronitromethane	TCNM	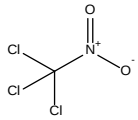	164.5	–	112	105800
Bromonitromethane	BNM	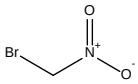	140.0	7.56	147.472	18680
Dibromonitromethane	DBNM	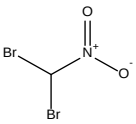	219.0	6.08	152.7	4577
Tribromonitromethane	TBNM	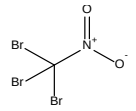	298.0	–	155.9	227.5
Bromochloronitromethane	BCNM	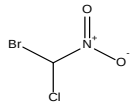	174.5	7.28	132.7	9163
Bromodichloronitromethane	BDCNM	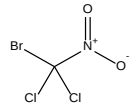	209.0	–	115.5	1007
Dibromochloronitromethane	DBCNM	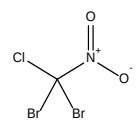	253.5	–	134.9	486.1

Table S2 Water quality indices of real water samples after 0.45 μm membrane filtration.

Source of water	DOC (mg/L)	UV_{254} (cm^{-1})	pH	CODcr (mg/L)	NH_4^+-N (mg/L)	NO_3^--N (mg/L)	TN (mg/L)	Br^- (mg/L)	Cu (mg/L)
Wastewater treatment plant	8.57	0.064	7.50	12.00	0.10	6.51	6.79	0.25	–
Water supply plant	3.58	0.026	7.64	0.79	0.03	1.50	1.85	0.12	0.0011

Notes: The real water samples were collected between filtration and disinfection from the wastewater treatment plant (WTP) and water supply plant (WSP) in Nanjing (China) and filtered through 0.45-μm membrane filters.

Table S3 The degradation of HNMs by LP-UV irradiation and ·OH.

HNMs	ε_{254} ($M^{-1}\cdot cm^{-1}$)	Φ_{254}	$k_f^{\#}$ (× 10^{-4} cm^2/mJ)	$k_{\cdot OH}$ (× 10^8 $M^{-1}\cdot s^{-1}$)
CNM	N.A.	N.A.	N.A.	1.96
BNM	N.A.	N.A.	N.A.	0.84
BCNM	N.A.	N.A.	N.A.	4.2
DCNM	N.A.	N.A.	N.A.	5.2
DBNM	N.A.	N.A.	N.A.	4.75
TCNM	31.9	0.48	0.75	0.64
BDCNM	228	0.52	5.8	1.16
DBCNM	525	0.54	13.7	1.65
TBNM	729	0.59	20.8	2.38

Notes: N.A. represents not available. ε is the molar absorption coefficient for HNMs ($M^{-1}\cdot cm^{-1}$); Φ is the quantum yield; k_f is the photolysis rate constants (Mezyk et al., 2006; Cole et al., 2007; Chuang et al., 2016; Zhang et al., 2019; Lei et al., 2021).

Table S4 The information on the possible intermediates.

Molecular formulas	Structure	Weight	m/z
$C_4H_6ClNO_4$	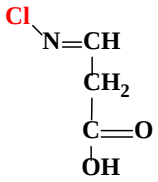	167	167.5
$CNOCl_3$	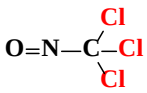	147	148
CH_2NOBr	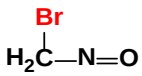	124	125
$CHNOBr_2$	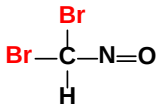	203	203.1
$C_2H_2O_3$	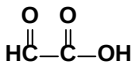	74	74

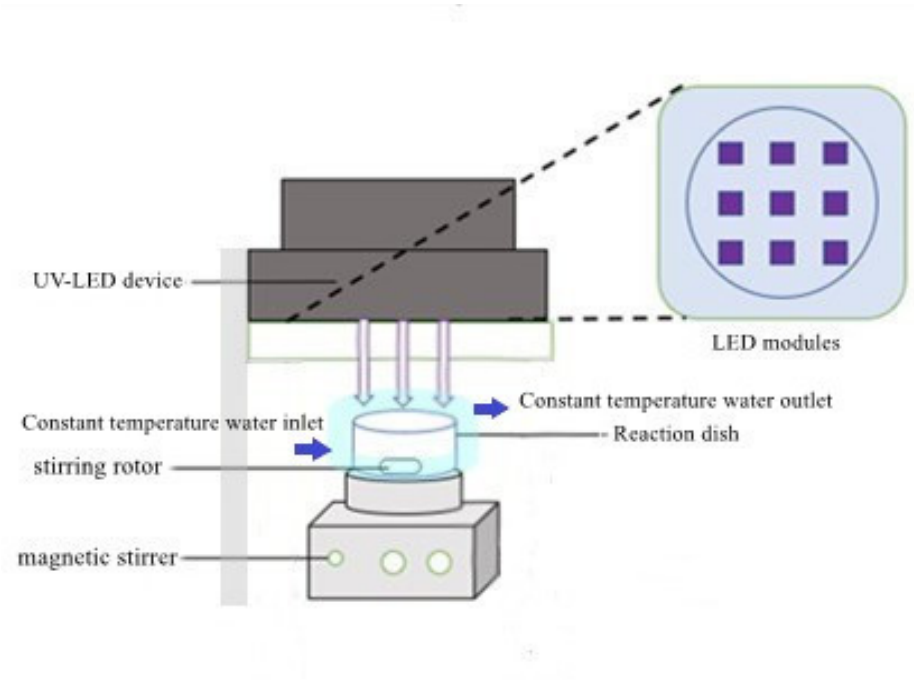

Fig. S1 Illustration of the experimental set-up. The structure of the LED-UV_{265} device was presented in Fig. S2. The wavelength of LED-UV was 265 nm (Fig. S3). The reaction device (1000 mL) was a double-layer cylindrical quartz reactor (24.0 cm height, 15.0 cm diameter, 2.0 cm wall thickness).

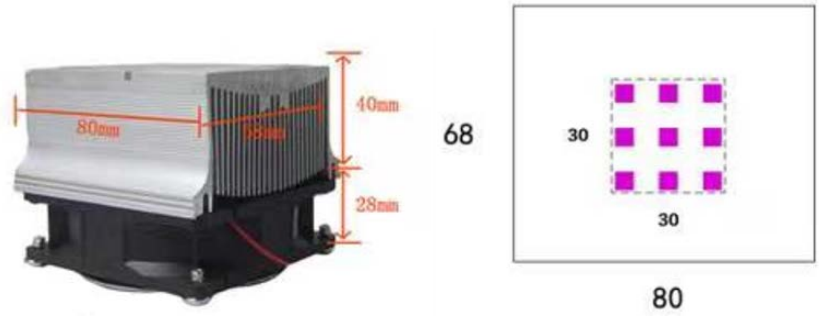

Fig. S2 Structure of the LED-UV_{265}.

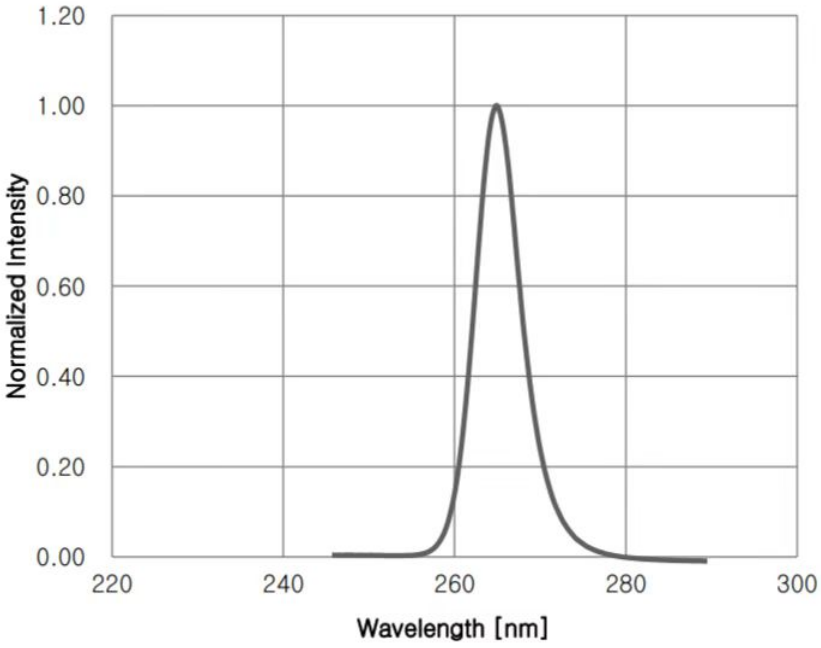

Fig. S3 Wavelength of the LED-UV.

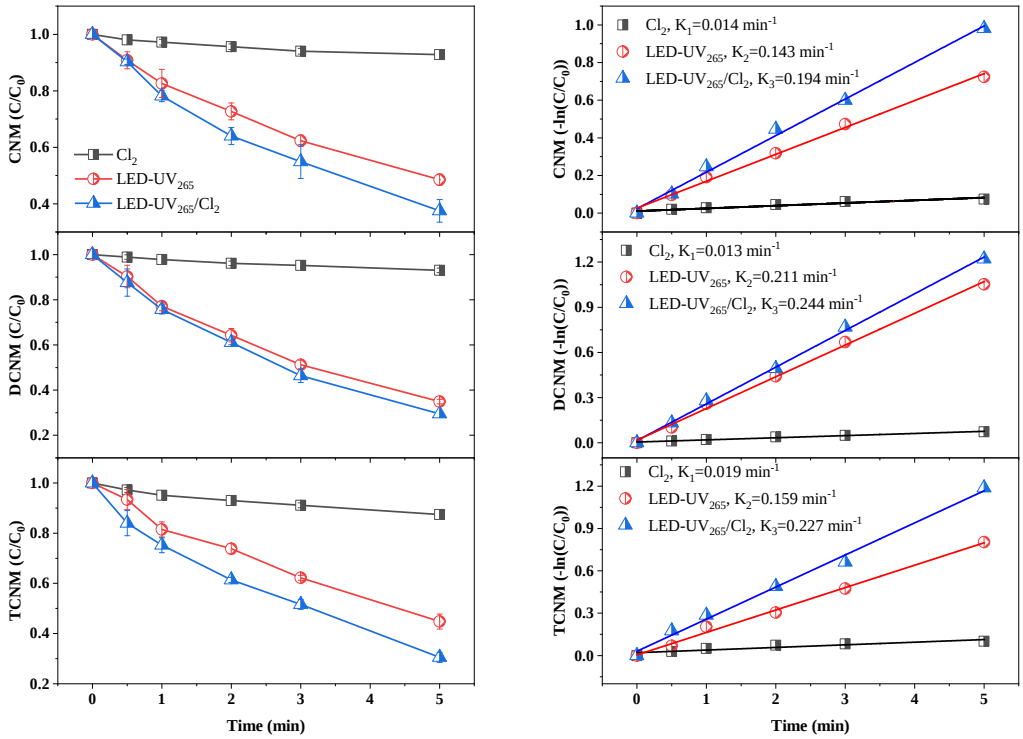

Fig. S4 Degradation efficiencies and kinetics of CNM, DCNM, and TCNM under chlorine, LED-UV_{265} and LED-UV_{265}/chlorine. Experimental conditions: [CNM] = 200 μg/L, [DCNM] = 200 μg/L, [TCNM] = 200 μg/L, [free chlorine] = 1.5 mg/L, pH = 7.0. [UV_{265} intensity] = 0.61 mW/cm^2.

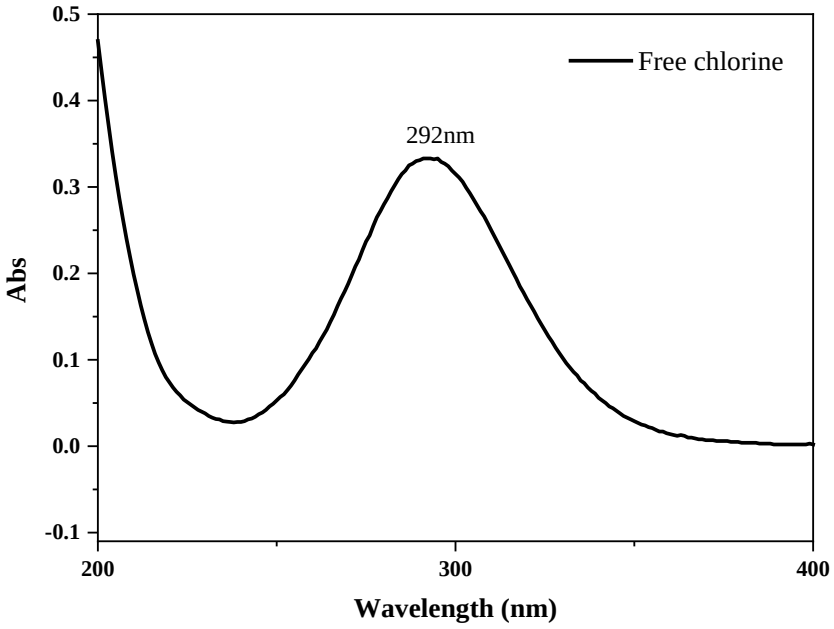

Fig. S5 Absorption spectra of free chlorine (t = 20℃, 50 mg/L free chlorine, pH = 7.0).

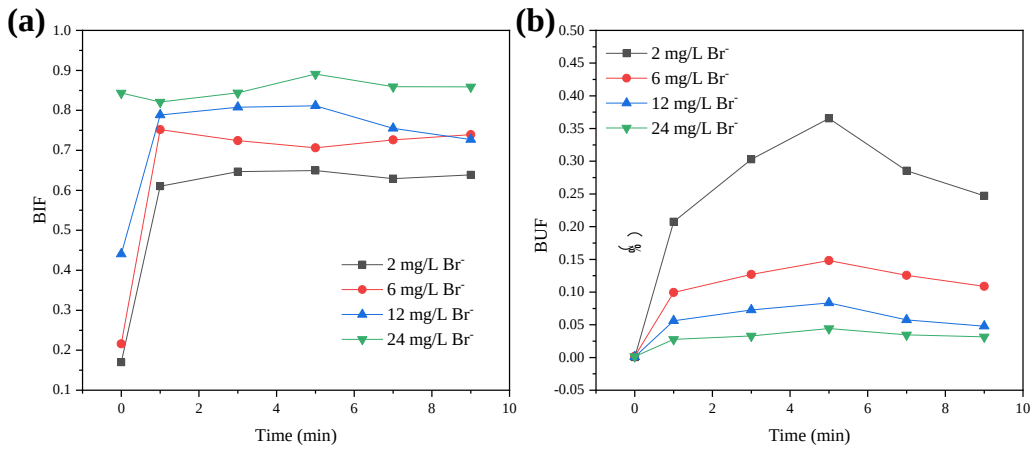

Fig. S6 Effect of Br^- concentrations on BIF (a) and BUF (b) of HNMs. Conditions: [ASP] = 2 mmol/L, [free chlorine] = 10 mg/L, [UV_{265} intensity] = 0.61 mW/cm^2, pH = 7.0.

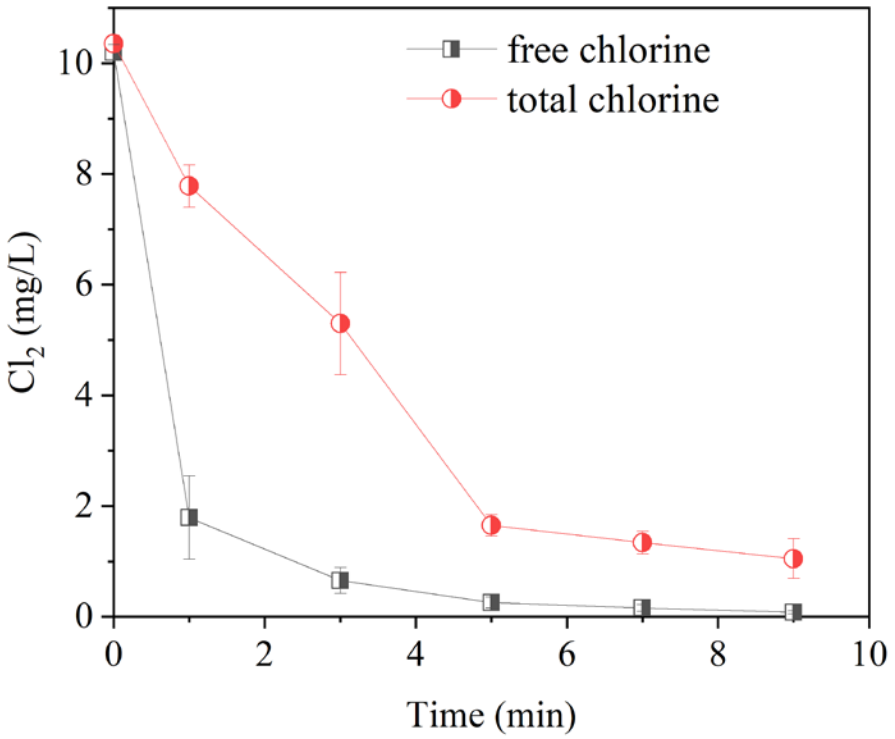

Fig. S7 Different forms of chlorine. Conditions: [ASP] = 2 mmol/L, [UV_{265} intensity] = 0.61 mW/cm^2, pH = 7.0.

References

Chuang Y H, Parker K M, Mitch W A (2016). Development of predictive models for the degradation of halogenated disinfection byproducts during the UV/H_2O_2 advanced oxidation process. Environmental Science & Technology, 50(20): 11209–11217

Cole S K, Cooper W J, Fox R V, Gardinali P R, Mezyk S P, Mincher B J, O'shea K E (2007). Free radical chemistry of disinfection byproducts. 2. Rate constants and degradation mechanisms of trichloronitromethane (chloropicrin). Environmental Science & Technology, 41(3): 863–869

How Z T, Kristiana I, Busetti F, Linge K L, Joll C A (2017). Organic chloramines in chlorine-based disinfected water systems: A critical review. Journal of Environmental Sciences-China, 58: 2–18

Lei X, Lei Y, Zhang X, Yang X (2021). Treating disinfection byproducts with UV or solar irradiation and in UV advanced oxidation processes: A review. Journal of Hazardous Materials, 408: 124435

Mezyk S P, Helgeson T, Cole S K, Cooper W J, Fox R V, Gardinali P R, Mincher B J (2006). Free radical chemistry of disinfection-byproducts. 1. Kinetics of hydrated electron and hydroxyl radical reactions with halonitromethanes in water. Journal of Physical Chemistry A, 110(6): 2176–2180

Zhang Y, Xiao Y, Zhang Y, Lim T T (2019). UV direct photolysis of halogenated disinfection byproducts: Experimental study and QSAR modeling. Chemosphere, 235: 719–725